# Kinetic Schemes in the case of low Mach numbers

Michael Junk

Institut für Techno–
und Wirtschaftsmathematik
Erwin–Schrödingerstraße,
67663 Kaiserslautern, Germany

e–mail: junk@itwm.uni-kl.de

1

## Abstract

Originally, Kinetic Schemes have been used as numerical methods to solve the system of compressible Euler equations in gas dynamics. The main idea in the approach is to construct the numerical flux function based on a microscopical description of the gas. In this article the schemes are investigated in the case of isentropic Euler equations and low Mach numbers. Expanding the microscopical velocity distribution naturally leads to new Kinetic Schemes with strong resemblance to Lattice Boltzmann methods. By adjusting the parameters of the Kinetic Scheme the numerical viscosity can be used to reproduce a given physical viscosity. In this way, a finite difference solver for the incompressible Navier–Stokes equation is obtained. Its close relation to the Lattice Boltzmann approach is highlighted.

# 1 Introduction

Generally speaking, Kinetic Schemes are numerical methods to solve systems of hyperbolic conservation laws. To explain the basic idea, we consider the paradigmatic case of gas dynamics. The classical derivation of the governing evolution equations relies on a continuum model of a gas in a state of local thermodynamical equilibrium. The Euler equations for densities of mass $\rho$, momentum $\rho u$ and energy $E$ are then obtained by applying conservation principles [3].

A second and more general description is obtained with Gas–Kinetic theory. In this approach, the state variable is a particle distribution function $f(x, v, t)$ which specifies the density of microscopic gas particles with velocity $v$ at time $t$ and position $x$. The evolution of $f$ is given by Boltzmann equation [4]. Physically, the basic quantities $\rho, \rho u, E$ of the macroscopic approach can be recovered from $f$ by taking velocity averages of the corresponding microscopic mass, momentum and energy densities $f, vf, \frac{1}{2}\|v\|^2 f$. A mathematical connection between the two descriptions is obtained in the so called hydrodynamical limit where particle collisions become dominant. In this asymptotic case, solving Boltzmann equation is equivalent to solving Euler equations. This is possible because the particle distribution function $f$ attains a very special functional form: as a function of $v$ it is a Maxwellian distribution

$$\mathcal{M}(v) = \frac{\rho}{(2\pi)^{\frac{d}{2}} c^d} \exp\left(-\frac{|v - u|^2}{2c^2}\right),$$

$$c^2 = \frac{p}{\rho}, \quad p = \frac{2}{3}\left(E - \frac{1}{2}\rho|u|^2\right), \quad v \in \mathbb{R}^d. \tag{1}$$

and the $(x, t)$–dependence enters only through the parameters $\rho, u, E$ which are solutions of the Euler system. (We assume a $d$ dimensional velocity space.)

In Kinetic Schemes, the relation between the two models is used to obtain a scheme for the Euler system. Given a macroscopic state $\rho, u, E$ depending on space and time, the idea is to set up a continuum of microscopic particles whose velocity distribution is given by the equilibrium distribution (1). The Boltzmann evolution is then approximated by a splitting approach which separates transport from collisions. First, the particles move freely in space according to their prescribed velocities. In this process, the macroscopic parameters $\rho, u$ and $E$ also evolve in time. However, the velocity distribution deviates more and more from the equilibrium form so that equivalence between Boltzmann and Euler description is no longer given. Therefore, transport is stopped after a small time step and collisions are assumed to take place. In general, this collision process is a complicated procedure but in the limit of dominating

3

collisions this step is just a projection of the distribution function into equilibrium form. Since the parameters $\rho, u, E$ are invariant under collisions, they keep their values which resulted from the transport step. With the distribution function back in equilibrium form, the whole process is then iterated to obtain an approximation at larger times.

A very similar approach is given by Lattice Boltzmann methods which also employ the evolution of microscopic gas models to approximate macroscopic equations of fluid dynamics. Compared to Kinetic Schemes which have been designed for the hydrodynamical limit, Lattice Boltzmann methods rather work in a diffusion limit so that they approximate incompressible Navier–Stokes equations. While the Lattice Boltzmann approach is based on simple, discrete gas models, Kinetic Schemes can be formulated with a wide variety of equilibrium distributions and space discretizations. As we will see below, Kinetic Schemes based on discrete equilibrium distributions applied in low Mach number flows can be viewed as building blocks of the Lattice Boltzmann method.

In 1974, the first Kinetic Scheme has been presented by Sanders and Prendergast [29]. The chosen distribution function is not a Maxwellian but a weighted sum of Dirac deltas. A modification and extension of this discrete equilibrium distribution function will be the basis for Kinetic Schemes in Lattice Boltzmann form presented below. A few years later, an approach to construct Kinetic Schemes for general hyperbolic systems of conservation laws is described in a review paper by Harten, Lax and van Leer [12] where the schemes are called Boltzmann-type schemes. In the 80's, Kinetic Schemes based on the Maxwellian distribution have been analyzed by several authors [24, 28, 7, 6]. Kaniel investigates a Kinetic Scheme for the isentropic Euler equations [15, 18, 27] based on yet another distribution function. A general approach to construct Kinetic Schemes for the Euler system has been introduced by Perthame in [21]. In [17], Kinetic Schemes for moment systems proposed by Levermore and Anile are constructed. Also, a new approach is presented which allows the construction of consistent Kinetic Schemes for general systems of conservation laws. It is a generalization of the scalar case which has been analyzed in [2, 11, 22].

In the following we will focus on the case of isentropic Euler equations

$$
\begin{aligned}
&\partial_t \rho + \operatorname{div}(\rho u) = 0, \\
&\partial_t(\rho u) + \operatorname{div}(\rho u \otimes u) + \nabla p(\rho) = 0.
\end{aligned}
\tag{2}
$$

which is a hyperbolic system if the sound speed

$$
c_s(\rho) = \sqrt{p'(\rho)}
$$

4

is real. In order to set up a Kinetic Scheme for (2), a natural particle distribution function is the Maxwellian (1) where now the given pressure law $p(\rho)$ is used

$$\mathcal{M}(\rho, u; v) = \frac{\rho}{(2\pi)^{\frac{d}{2}} c^d} \exp\left(-\frac{|v - u|^2}{2c^2}\right).$$

In the case of perfect gases for which

$$p(\rho) = A\rho^\gamma, \qquad \gamma \geq 1,$$

the velocity parameter $c(\rho) = \sqrt{p(\rho)/\rho}$ and the sound speed $c_s$ are related by

$$c_s = \sqrt{\gamma}\, c.$$

In particular, for $\gamma = 1$ the velocities coincide and are independent of $\rho$. The corresponding pressure law $p(\rho) = c_s^2 \rho$ is called *isothermal* in view of the state equation $p = R\theta\rho$ which connects density and pressure with the absolute temperature $\theta$ ($R > 0$ is the gas constant). We will mainly consider the isothermal case because it is the simplest choice and in the low Mach number limit the actual form of the pressure law is irrelevant.

In Section 2, Kinetic Schemes are introduced based on a general class of distribution functions which contains the Maxwellian as a special case. Then, an expansion of the distribution functions gives rise to new schemes which are shown to be consistent to (2). Analyzing the modified equations for these schemes in a low Mach number limit eventually shows that the Kinetic Schemes yield approximate solutions to the incompressible Navier Stokes equation. In Section 5 a particular scheme is analyzed and finally relations to Lattice Boltzmann methods are highlighted.

## 2    The Kinetic Scheme

To motivate the definition of Kinetic Schemes we use a formal argument which can be made precise for scalar conservation laws [19]. Let us assume that $F(x, v, t)$ is the solution of a Boltzmann like equation

$$\partial_t F + v_i \partial_{x_i} F = Q \tag{3}$$

where $Q$ satisfies

$$\langle Q, 1 \rangle_v = 0, \qquad \langle Q, v \rangle_v = 0$$

(we use Einstein's summation convention and $\langle \cdot, \cdot \rangle_v$ denotes integration with respect to $v$). Moreover, $Q$ is supposed to constrain $F$ to the special $v$–dependence $F(x, v, t) = \mathcal{M}(\rho(x, t), u(x, t); v)$ where $\mathcal{M}$ is the Maxwellian. We

5

note that
$$\langle \mathcal{M}(\rho, u; v), 1 \rangle_v = \rho,$$
$$\langle \mathcal{M}(\rho, u; v), v_i \rangle_v = \rho u_i, \tag{4}$$
$$\langle \mathcal{M}(\rho, u; v), v_i v_j \rangle_v = \rho u_i u_j + p(\rho)\delta_{ij},$$

Multiplying (3) with $\begin{pmatrix} 1 \\ v \end{pmatrix}$ and integrating over $v$ we obtain with $U(x,t) = (\rho(x,t), u(x,t))$

$$\partial_t \left\langle \mathcal{M}(U(x,t); v), \begin{pmatrix} 1 \\ v \end{pmatrix} \right\rangle_v + \partial_{x_i} \left\langle \mathcal{M}(U(x,t); v), v_i \begin{pmatrix} 1 \\ v \end{pmatrix} \right\rangle_v = 0.$$

which is exactly the isentropic Euler system due to (4). This relation between kinetic and macroscopic equation can be used to set up a numerical scheme. In order to approximate the evolution (3) we enforce the constraint given through $Q$ not continuously but only at discrete points in time. More precisely, we neglect the if $U^0(x)$ is the given initial value, we consider the solution of the resulting free transport equation

$$\partial_t F + v_i \partial_{x_i} F = 0, \qquad F(x, v, 0) = \mathcal{M}(U^0(x); v)$$

which is just

$$F(x, v, t) = \mathcal{M}(U^0(x - vt); v).$$

Since $v$ appears in the argument of $U^0$, the distribution function increasingly deviates from a Maxwellian for growing $t$ (which is the consequence of neglecting $Q$). Hence, the moment vector

$$\begin{pmatrix} \rho(x,t) \\ \rho u(x,t) \end{pmatrix} = \left\langle \mathcal{M}(U^0(x - vt); v), \begin{pmatrix} 1 \\ v \end{pmatrix} \right\rangle_v \tag{5}$$

satisfies (2) only up to some error term which also grows in time. To control the error, the free flow is stopped after some small time step $\Delta t$ and the constraint

$$\mathcal{M}(U^0(x - v\Delta t); v) \longrightarrow \mathcal{M}(U(x, \Delta t); v)$$

is enforced with $U(x, \Delta t) = (\rho(x, \Delta t), u(x, \Delta t))$ defined in (5). Iterating this process, we get the scheme

$$\begin{pmatrix} \rho^{n+1}(x) \\ \rho^{n+1} u^{n+1}(x) \end{pmatrix} = \left\langle \mathcal{M}(U^n(x - v\Delta t); v), \begin{pmatrix} 1 \\ v \end{pmatrix} \right\rangle_v, \qquad n \in \mathbb{N}_0.$$

Of course, a discretization in space is also necessary to obtain a numerical code.

6

As important observation we note that the only structural features of $\mathcal{M}$ we have used are the moment conditions. In particular, we can replace $\mathcal{M}(\rho, u; v)$ by any other function $f(\rho, u; v)$ which satisfies

$$
\begin{aligned}
\langle f(\rho, u; v), 1 \rangle_v &= \rho, \\
\langle f(\rho, u; v), v_i \rangle_v &= \rho u_i, \\
\langle f(\rho, u; v), v_i v_j \rangle_v &= \rho u_i u_j + p(\rho) \delta_{ij},
\end{aligned}
\tag{6}
$$

The corresponding Kinetic Scheme then reads

$$
\begin{pmatrix} \rho^{n+1}(x) \\ \rho^{n+1} u^{n+1}(x) \end{pmatrix} = \left\langle f(U^n(x - v\Delta t); v), \begin{pmatrix} 1 \\ v \end{pmatrix} \right\rangle_v, \quad U^n = (\rho^n, u^n).
\tag{7}
$$

For a quite general class of distribution functions $f$ the $(\rho, u)$ dependence is of the form

$$
f(\rho, u; v) = \frac{\rho}{c^d} f^* \left( \frac{v - u}{c} \right)
$$

where $f^*$ is a non negative, symmetric measure which is normalized in the sense

$$
\begin{aligned}
\langle f^*(v), 1 \rangle_v &= 1, \\
\langle f^*(v), v_i v_j \rangle_v &= \delta_{ij}.
\end{aligned}
\tag{8}
$$

An isotropy condition on the fourth order moments

$$
\langle f^*(v), v_i v_j v_k v_l \rangle_v = \lambda \left( \delta_{ij} \delta_{kl} + \delta_{ik} \delta_{jl} + \delta_{il} \delta_{kj} \right)
\tag{9}
$$

is not required for classical Kinetic Schemes but it will be important in the low Mach number case considered below.

We note that with

$$
f^*(v) = \frac{1}{(2\pi)^{\frac{d}{2}}} \exp \left( -\frac{1}{2} |v|^2 \right)
\tag{10}
$$

the Maxwellian belongs to the above class of distribution functions, satisfying $\lambda = 1$. Another example is based on the suitably normalized characteristic function of the $d$–dimensional ball

$$
f^*(v) = \frac{\Gamma\left(\frac{d}{2}\right) d}{2(\sqrt{(d+2)\pi})^d} \mathcal{X}_{[0, \sqrt{d+2}]}(|v|).
\tag{11}
$$

The approach based on this distribution function has been analyzed at length in [15, 18]. The fourth order tensor in (9) is characterized by $\lambda = \frac{d+2}{d+4}$.

Finally, we are especially interested in discrete distribution functions like

$$
f^*(v) = \left( 1 - \frac{2}{\sigma^2} \right) \delta(v) + \frac{1}{n\sigma^2} \sum_{l=1}^{2n} \delta(v - \sigma e_l)
\tag{12}
$$

7

for the two dimensional case, where $\sigma > \sqrt{2}$, $n \geq 2$ and $e_l$ are unit vectors of the form

$$e_l = \begin{pmatrix} \cos\left(l\frac{\pi}{n}\right) \\ \sin\left(l\frac{\pi}{n}\right) \end{pmatrix}, \qquad l = 1, \ldots, 2n.$$

For the full Euler system, the case $n = 2$ has been mentioned in [29]. For our purpose, however, the case $n = 3$ will be most important because it leads to a simple Kinetic scheme which operates on a hexagonal grid similar to Lattice Boltzmann methods in 2D [5]. We note that for $n = 2$ the fourth order tensor is not of the form (9) since $\langle f^*(v), v_1^2 v_2^2 \rangle_v = 0$ but $\langle f^*(v), v_1^4 \rangle_v \neq 0$ (which excludes this particular case from the low Mach number expansion below). For all larger $n$ we obtain (9) with $\lambda = \sigma^2/4$. Another choice which is related to widely used Lattice Boltzmann schemes [1, 14] is given by the nine velocity distribution

$$f^*(v) = \eta f_1^*(v) + (1 - \eta) f_2^*(v), \qquad \eta \in (0, 1) \tag{13}$$

While $f_1^*$ is of the form (12) with $n = 2$ (velocities pointing in coordinate directions), $f_2^*$ has the structure

$$f_2^*(v) = \left(1 - \frac{1}{\sigma^2}\right) \delta(v) + \frac{1}{4\sigma^2} \sum_{l=1}^{4} \delta(v - \sqrt{2}\sigma e_l'),$$

with discrete velocities in diagonal directions

$$e_l' = \begin{pmatrix} \cos\left((l - \frac{1}{2})\frac{\pi}{2}\right) \\ \sin\left((l - \frac{1}{2})\frac{\pi}{2}\right) \end{pmatrix}.$$

The convex combination yields a symmetric $f^*$ which satisfies the normalization conditions (8). If $\eta = \frac{2}{3}$ we even get isotropy (9) with $\lambda = \sigma^2/3$.

# 3   Velocity distribution at low Mach numbers

In situations where the speed $|u|$ of the flow is much smaller than the velocity parameter $c = \sqrt{p/\rho}$, the distribution function

$$f(\rho, u; v) = \frac{\rho}{c^d} f^*\left(\frac{v}{c} - \frac{u}{c}\right) \tag{14}$$

is only a small perturbation of

$$f(\rho, 0; v) = \frac{\rho}{c^d} f^*\left(\frac{v}{c}\right).$$

8

For perfect gases, the parameter $M = |u|/c$ is proportional to the Mach number

$$Ma = \frac{|u|}{c_s} = \frac{|u|}{\sqrt{\gamma}c} = \frac{1}{\sqrt{\gamma}}M.$$

For more general pressure laws where only $p(0) = 0$ and convexity of $p$ is assumed, we still have the relationship $Ma \leq M$. The case $M \ll 1$ therefore corresponds to small Mach number flows. The derivations in this section are done for the isothermal case ($\gamma = 1$) where $c = c_s$ and $Ma = M$. We briefly comment on more general laws at the end of the section.

To motivate the following low Mach number expansion of $f(\rho, u; v)$ let us briefly consider the case (12). With $\sigma = 2$, $n = 3$, $f(\rho, u; v)$ is of the form

$$f(\rho, u; v) = \frac{\rho}{2}\delta(v - u) + \frac{\rho}{12}\sum_{l=1}^{6}\delta(v - (2c_s e_l + u)).$$

To investigate the Kinetic Scheme based on this velocity distribution we consider how information is transported during the free flow step. After a time $\triangle t$ the state at position $x$ influences the points

$$x_0 = x + \triangle t u, \qquad \text{and} \qquad x_l = x + \triangle t(2c_s e_l + u), \quad l = 1, \ldots, 6$$

or using the abbreviations $\triangle x = 2c_s \triangle t$ and $e_0 = 0$

$$x_l = x + \triangle x e_l + \triangle x \frac{u}{2c_s} \quad l = 1, \ldots, 6.$$

In the case $Ma = |u|/c_s \ll 1$, information is essentially transported to the neighboring points $x + \triangle x e_l$ on a hexagonal grid (see Figure 1) whereas for $Ma = \mathcal{O}(1)$ an immediate correlation between the points $x_l$ and the grid is no longer visible.
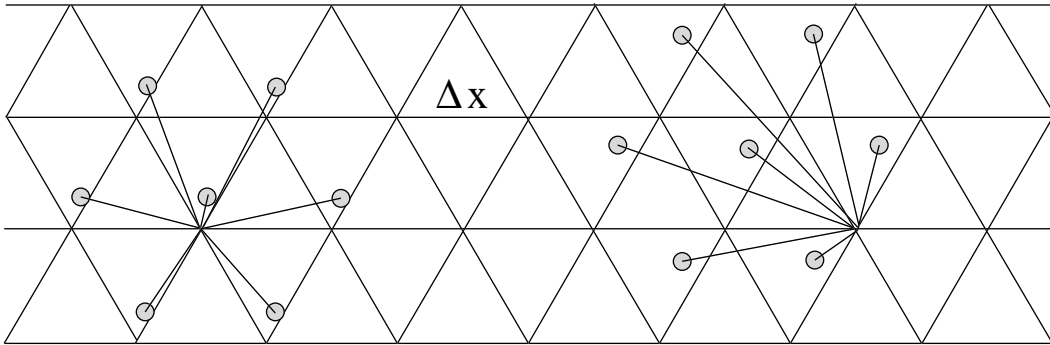


Figure 1: $|u|/c_s \ll 1$ (left) and $|u|/c_s \sim 1$ (right)

9

In other words, if $|u|/c_s$ ranges in the unit circle, information is transported to any point of the right shaded area in Figure 2. The underlying hexagonal structure is still visible but it becomes less and less important if we allow for larger values of $u/c_s$. Conversely, if $u/c_s \to 0$, it seems to be worthwhile to use the emerging hexagonal structure in space.
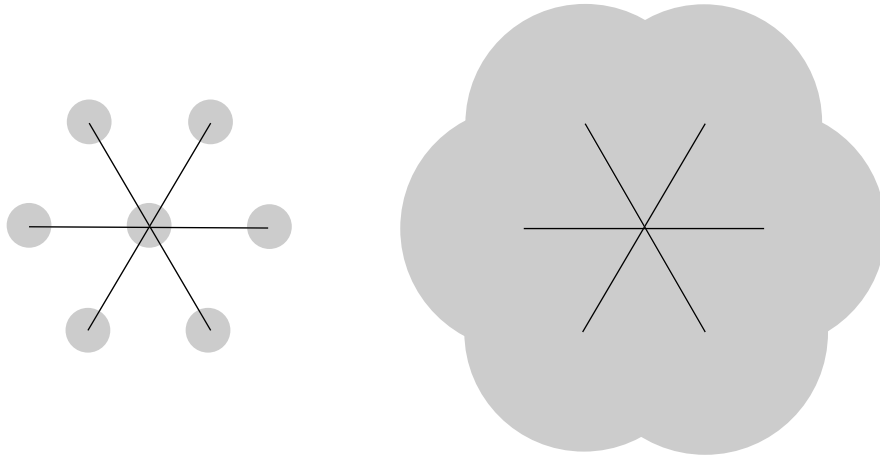


Figure 2: Range of influence for varying $u$

The idea is to base the scheme on $f(\rho, 0; v)$ so that information travels exactly to neighboring points on the grid. The neglected small deviation due to $|u|/c_s \ll 1$ is taken into account by a polynomial perturbation. Altogether, $f$ will be replaced by $h(\rho, u; v) = \omega(u; v) f(\rho, 0; v)$ with a suitable $v$–polynomial $\omega$. In contrast to the original function $f$, the perturbation is non negative only for a restricted velocity range. Also, the $u$ dependence of the perturbation no longer reflects translational invariance like the one of $f$. These disadvantages, which are of minor importance for moderate flow situations at low Mach numbers, are the prize to pay for the simplification of the scheme.

In the isothermal case, we have the following result:

> *If $f^*$ is a non-negative symmetric measure on $\mathbb{R}^d$ which satisfies (8) and (9) then a low Mach number approximation of $f(\rho, u; v) = \rho f^*((v - u)/c_s)/c_s^d$ is given by*
>
> $$h(\rho, u; v) = \omega(u; v) f(\rho, 0; v) \qquad (15)$$
>
> *with a polynomial*
>
> $$\omega(u; v) = 1 + \frac{u \cdot v}{c_s^2} + \frac{1}{2} \left( \frac{1}{\lambda} \frac{(u \cdot v)^2}{c_s^4} - \beta \left( \frac{\lambda - 1}{\lambda} \frac{|v|^2}{c_s^2} + 2 \right) \frac{|u|^2}{c_s^2} \right)$$
> $$(16)$$

10

and $\beta = 1/((d+2)\lambda - d)$. The new distribution function $h$ satisfies the moment conditions (6). If $\lambda \leq 1$, $h$ is non-negative provided

$$Ma^2 = \frac{|u|^2}{c_s^2} \leq \frac{1}{2\beta}. \tag{17}$$

For $\lambda > 1$, non-negativity of $h$ can only be obtained if $f^*$ has a bounded velocity support in $|v| \leq v_{max}$. Under this restriction we find $h \geq 0$ if

$$Ma^2 \leq \frac{1}{2} \left( \frac{\lambda - 1}{2\lambda} v_{max}^2 (1 + \beta) + \beta \right)^{-1}. \tag{18}$$

For the Maxwellian (10) we have already mentioned that $\lambda = 1$ so that $\beta = 1/2$. Consequently, the low Mach number approximation of the Maxwellian violates the physical positivity restriction on particle distribution functions for $Ma \geq 1$. Practically, one observes instabilities of the Kinetic Scheme if $h \geq 0$ is violated so that the positivity considerations indicate the stability range of the scheme.

The construction of $h$ is based on two requirements. First, $h$ should satisfy the moment conditions (6) so that it is applicable in Kinetic Schemes. Second, integrals over $h$ should be easy to evaluate so that the scheme can be efficiently implemented.

Since the right hand sides of (6) involve at most quadratic expressions in $u$, an expansion in $u/c_s$ up to second order around $u = 0$ leaves the right hand sides unchanged. Consequently, the expansion of $f(\rho, u; v)$ to the same order

$$g(\rho, u; v) = \frac{\rho}{c_s^d} \left( 1 - \frac{u_j}{c_s} \partial_{w_j} + \frac{1}{2} \frac{u_i u_j}{c_s^2} \partial_{w_i} \partial_{w_j} \right) f^*(w) \Big|_{w = \frac{v}{c_s}}. \tag{19}$$

still satisfies (6). A disadvantage of (19) is that derivatives of $f^*$ are involved. In particular, if $f^*$ is not very regular, the expansion $g$ has to be interpreted as a generalized function. (For discrete measures like (12) or (13), $g$ contains derivatives of Dirac delta distributions.) In order to simplify the structure of $g$, we use the observation that $\partial_{w_j} f^*(w)$ acts exactly like $-w_j f^*(w)$, at least on second order polynomials (which are the most important test functions used in the derivation of the Kinetic Scheme). Indeed, if

$$P(w) = a + a_i w_i + a_{ik} w_i w_k, \qquad w \in \mathbb{R}^d$$

is any quadratic polynomial we find with (8) and the symmetry of $f^*$

$$\begin{aligned}
\left\langle \partial_{w_j} f^*(w), P(w) \right\rangle_w &= - \left\langle f^*(w), \partial_{w_j} P(w) \right\rangle_w \\
&= - \left\langle f^*(w), a_j + (a_{ij} + a_{ji}) w_i \right\rangle_w = -a_j.
\end{aligned}$$

11

On the other hand,

$$\langle w_j f^*(w), P(w)\rangle_w = \langle f^*(w), aw_j + a_i w_i w_j + a_{ik} w_i w_j w_k\rangle_w$$
$$= \langle f^*(w), a_i w_i w_j\rangle_w = a_j.$$

Hence, for all quadratic polynomials $P$

$$\langle \partial_{w_j} f^*, P\rangle_w = \langle -w_j f^*, P\rangle_w.$$

Similarly, we obtain with $\beta = 1/((d+2)\lambda - d)$

$$\langle \partial_{w_j}\partial_{w_i} f^*, P\rangle_w = \left\langle \left(\frac{1}{\lambda}w_i w_j - \beta\left(\frac{\lambda-1}{\lambda}|w|^2 + 2\right)\delta_{ij}\right) f^*, P\right\rangle_w.$$

Using these representations in (19), we recover the distribution $h(\rho, u; v) = \omega(u; v)f(\rho, 0; v)$ with $\omega$ of the form (16). The distribution $h$ satisfies the moment conditions (6) since the same holds for $g$ and only quadratic polynomials are involved.

To check positivity of $h$, we start with the observation that

$$0 < \langle f^*(v), |v|^4\rangle = 3d\lambda + d(d-1)\lambda = d(d+2)\lambda.$$

To show positivity of $\beta$ we need the Schwarz inequality for the scalar product $(P, Q) \longrightarrow \langle f^*(v), P(v)Q(v)\rangle_v$

$$d = \langle f^*(v), |v|^2\rangle < \left(\langle f^*(v), 1\rangle \langle f^*(v), |v|^4\rangle\right)^{\frac{1}{2}} = \sqrt{d(d+2)\lambda}.$$

Taking squares and dividing by $d$

$$\frac{1}{\beta} = (d+2)\lambda - d > 0.$$

After regrouping (16) we obtain

$$\omega(u; v) = \frac{1}{2} - \beta\frac{|u|^2}{c_s^2} + \frac{1}{2}\left(\frac{u \cdot v}{c_s^2} + 1\right)^2 + \frac{1-\lambda}{2\lambda}\left(\frac{(u \cdot v)^2}{c_s^4} + \beta\frac{|u|^2|v|^2}{c_s^4}\right).$$

In the case $1 - \lambda \geq 0$ we see that $\omega(u; v) \geq \omega(u; 0)$. Requiring $\omega(u; 0) \geq 0$ then leads to the condition

$$Ma^2 = \frac{|u|^2}{c_s^2} \leq \frac{1}{2\beta}.$$

12

For $\lambda > 1$ the situation is more complicated. Inserting a velocity vector which is perpendicular to $u \neq 0$, we get

$$\omega(u; v) = 1 - \beta \frac{|u|^2}{c_s^2} \left( 1 + \frac{\lambda - 1}{2\lambda} \frac{|v|^2}{c_s^2} \right), \qquad v \perp u$$

which certainly becomes negative for very large $|v|$. However, the polynomial $\omega$ is only used in conjunction with the distribution function $f(\rho, 0; v)$. If $f^*$ has bounded support, say on $|v| \leq v_{\max}$, then $f(\rho, 0; v) = \frac{\rho}{c_s^d} f^*(\frac{v}{c_s})$ is supported on $c_s v_{\max}$. Since $(u \cdot v)^2 \leq |u|^2 |v|^2$ we then get

$$\frac{(u \cdot v)^2}{c^4} + \beta \frac{|u|^2 |v|^2}{c^4} \leq \frac{|u|^2 v_{\max}^2}{c^2} (1 + \beta),$$

so that $\omega(u; v) \geq 0$ provided $|v| \leq c_s v_{\max}$ and

$$Ma^2 \leq \frac{1}{2} \left( \frac{v_{\max}^2 (\lambda - 1)}{2\lambda} (1 + \beta) + \beta \right)^{-1}.$$

We conclude the section by giving a few remarks. For more general pressure laws than $p(\rho) = c_s^2 \rho$ (isothermal case) a similar derivation can be carried out. If the changes in $c(\rho) = \sqrt{p(\rho)/\rho}$ are small with respect to a reference value $\bar{c}$ we expand in $u/\bar{c}$ around zero and in $c$ around $\bar{c}$. Since $c$ enters quadratically in the moment conditions (6) (via $p = c^2 \rho$), a second order expansion is sufficient. We again obtain a polynomial perturbation of the form

$$\bar{\omega}(\rho, u; v) \frac{\rho}{\bar{c}^d} f^* \left( \frac{v}{\bar{c}} \right).$$

where $\bar{\omega}$ has the same form as (16) with $c$ replaced by $\bar{c}$ plus the additional term

$$\beta \left( d - \frac{|v|^2}{\bar{c}^2} \right) \left( 1 - \frac{c(\rho)^2}{\bar{c}^2} \right).$$

If the full Euler system is considered, the additional energy variable gives rise to another moment condition which involves a third order polynomial. However, it is no problem to generalize the approach presented here also to that case.

## 4 Kinetic Schemes at low Mach numbers

To study the approximation properties of the Kinetic Scheme, we perform a *modified equation analysis* [13]. The basic idea of this approach is the following: the discrete evolution given by some approximation procedure typically deviates from the actual evolution which is to be calculated. Hence, the equation

13

satisfied by the approximation can be thought of as being the original equation plus a source term which describes the error production. The so obtained *modified* equation obviously yields important information about the numerical scheme because (at least the lowest order term of) the error production is included.

For the Kinetic Scheme (7) based on a distribution function $h$ of type (15) with isothermal pressure law we find

$$
\partial_t \rho + \operatorname{div}(\rho u) = 0,
$$
$$
\partial_t(\rho u_k) + \operatorname{div}(\rho u_k u) + c_s^2 \partial_{x_k} \rho = \frac{\lambda \triangle t c_s^2}{2} (\rho \Delta u_k + R_k) \tag{20}
$$

where

$$
R_k = \frac{1}{\lambda} \Bigg( (2\lambda - 1)\partial_{x_k} \operatorname{div} u + (\lambda - 1)(u_k \Delta \rho + 2 \operatorname{div}(u \partial_{x_k} \rho))
$$
$$
- \frac{1}{c_s^2} \partial_{x_i} \partial_{x_j} (\rho u_i u_j u_k) \Bigg). \tag{21}
$$

To check that (20) is the modified equation one has to show that the scheme (7) with $f$ replaced by $h$ approximates the solution of (20) to second order in $\triangle t$. The necessary Taylor expansions are omitted for brevity. We just remark that all time derivatives of the solution $(\rho, u)$ of (20) can be expressed in terms of space derivatives by using (20) which relates space and time derivatives. For the expansion of the Kinetic Scheme (7) it is important to note that derivatives with respect to $\triangle t$ also lead to space derivatives (since $h(x - v\triangle t; v)$ is the solution of the free transport equation $\partial_t F + v \cdot \nabla_x F = 0$ with initial value $F(x, v, 0) = h(x, v)$ again time derivatives and space derivatives are connected). Moreover, each time derivative produces a factor $v$ because $\triangle t$ appears only in the form $v \triangle t$. The corresponding $v$-integrals can then be calculated due to our knowledge of the velocity moments of $h$.

To investigate the dependence on the Mach number, we scale $x$ with a typical length $L$, $t$ and $\Delta t$ with $T$ and $u$ with $L/T$ so that (20) turns into

$$
\partial_t \rho + \operatorname{div}(\rho u) = 0,
$$
$$
\partial_t(\rho u_k) + \operatorname{div}(\rho u_k u) + \frac{1}{Ma^2} \partial_{x_k} \rho = \frac{\lambda \triangle t}{2Ma^2} (\rho \Delta u_k + R_k) \tag{22}
$$

14

where $Ma = L/(Tc_s)$ and

$$R_k = \frac{1}{\lambda}\Bigg((2\lambda - 1)\partial_{x_k}\operatorname{div} u + (\lambda - 1)(u_k\Delta\rho + 2\operatorname{div}(u\partial_{x_k}\rho))$$

$$- Ma^2\partial_{x_i}\partial_{x_j}(\rho u_i u_j u_k)\Bigg). \quad (23)$$

We now distinguish two limits. First, if $Ma > 0$ is fixed, then (22) converges to the Euler system (2) in the limit $\triangle t \to 0$. (Since (22) is just (2) with an error production of order $\triangle t$, the Kinetic Scheme is first order consistent to the Euler system if $Ma$ is a fixed positive number.) If, however, the Mach number vanishes also in such a way that the quotient $\triangle t/Ma^2$ converges to some positive constant, the scheme is no longer consistent to the inviscid equations. We investigate this second limiting case by considering the coupling

$$\triangle t = \frac{2}{\lambda Re}Ma^2 \quad (24)$$

where $Re > 0$ is any positive value. Under the additional assumption that all terms in the momentum equation of (22) are $\mathcal{O}(1)$ quantities we find $\nabla\rho = \mathcal{O}(Ma^2)$. Hence, we can assume that $\rho = \rho^{(0)} + Ma^2\bar\rho$ where $\rho^{(0)}$ is a constant (say $\rho^{(0)} = 1$) and $\bar\rho$ and its derivatives are $\mathcal{O}(1)$. Inserting this ansatz into equation (22), we find

$$\operatorname{div} u = \mathcal{O}(Ma^2),$$
$$\partial_t u_k + (u.\nabla)u_k + \partial_{x_k}\bar\rho = \frac{1}{Re}\Delta u_k + \mathcal{O}(Ma^2). \quad (25)$$

(The additional term (23) is of order $Ma^2$ because $\operatorname{div} u = \mathcal{O}(Ma^2)$ and all derivatives of $\rho$ are $\mathcal{O}(Ma^2)$ by assumption.) We conclude that in the coupled limit $\triangle t/Ma^2 \to 0$ the modified equation of the Kinetic Scheme is no longer a perturbation of the isentropic Euler system (as for the simple limit $\triangle t \to 0$). Since $\mathcal{O}(Ma^2) = \mathcal{O}(\triangle t)$, it turns out that the Kinetic Scheme approximates the incompressible Navier-Stokes equation in that limit to first order in $\triangle t$.

## 5   Numerical examples

To calculate approximate solutions of the incompressible Navier–Stokes equation in two dimensions we will use a Kinetic Scheme based on (12) with $n = 3$

$$f^*(v) = \left(1 - \frac{2}{\sigma^2}\right)\delta(v) + \frac{1}{3\sigma^2}\sum_{l=1}^{6}\delta(v - \sigma e_l). \quad (26)$$

15

$e_l$ are unit vectors in the hexagonal directions

$$e_l = \begin{pmatrix} \cos\left(l\frac{\pi}{3}\right) \\ \sin\left(l\frac{\pi}{3}\right) \end{pmatrix}, \qquad l = 1, \ldots, 6$$

and $\sigma^2 > 2$. $f^*$ satisfies the moment conditions (8) and (9) with $\lambda = \sigma^2/4$. To simplify notation, we introduce vectors $c_i = c_s \sigma e_i$ for $i = 0, \ldots, 6$ where $e_0$ is the zero vector. The weights of the $\delta$-measures in (26) are denoted

$$f_0^* = 1 - \frac{2}{\sigma^2}, \qquad \text{and} \qquad f_i^* = \frac{1}{3\sigma^2} \quad i = 1, \ldots, 6$$

so that $f(\rho, 0; v) = \rho f^*(v/c_s)/c_s^2$ can be written in the form

$$f(\rho, 0; v) = \sum_{i=0}^{6} \rho f_i^* \delta(v - c_i).$$

According to Section 3, a particle distribution based on $f^*$ which works in the low Mach number case can be written in the form $h(\rho, u; v) = \omega(u; v) f(\rho, 0; v)$ so that

$$h(\rho, u; v) = \sum_{i=0}^{6} h_i(\rho, u) \delta(v - c_i) \qquad h_i(\rho, u) = \rho f_i^* \omega(u; c_i). \qquad (27)$$

(Note that $\omega(u; v)\delta(v - c_i) = \omega(u; c_i)\delta(v - c_i)$.) In this example, the general form (16) of $\omega$ simplifies to

$$\omega(u; c_0) = \tilde{\omega}(\mu; e_0) = 1 - \frac{1}{\sigma^2 - 2}|\mu|^2,$$

$$\omega(u; c_i) = \tilde{\omega}(\mu; e_i) = 1 - \frac{1}{2}|\mu|^2 + \sigma\mu \cdot e_i + 2(\mu \cdot e_i)^2 \qquad i = 1, \ldots, 6$$

where $\mu = u/c_s$. Since $f^*$ is supported on a disk with radius $\sigma$, the considerations in Section 3 yield positivity of $h$ provided

$$Ma^2 \leq \frac{\sigma^2 - 2}{2}, \qquad 2 \leq \sigma^2 \leq 4 \qquad (28)$$

respectively

$$Ma^2 \leq \frac{1}{\sigma^2 - 3}, \qquad \sigma^2 > 4.$$

16

Plugging $h$ into definition (7) of the Kinetic Scheme, we get

$$\begin{pmatrix} \rho^{n+1}(x) \\ \rho^{n+1}u^{n+1}(x) \end{pmatrix} = \left\langle h(\rho^n(x - v\triangle t), u^n(x - v\triangle t); v), \begin{pmatrix} 1 \\ v \end{pmatrix} \right\rangle_v$$

$$= \sum_{i=0}^{6} \left\langle \delta(v - c_i), h_i(\rho^n(x - v\triangle t), u^n(x - v\triangle t)) \begin{pmatrix} 1 \\ v \end{pmatrix} \right\rangle_v$$

$$= \sum_{i=0}^{6} \begin{pmatrix} 1 \\ c_i \end{pmatrix} h_i(\rho^n(x - c_i\triangle t), u^n(x - c_i\triangle t))$$

Setting $\triangle x = c_s\sigma\triangle t$ we can write $c_i\triangle t = e_i\triangle x$ so that information to update the density in $x$ is only taken from neighboring points in the hexagonal directions $e_i$ and distance $\triangle x$. In particular, no additional space discretization is required if the data points are located on a hexagonal lattice. (Note that this property is related to the structure of $h$ and has been the main motivation for the derivation in Section 3.) We also remark that the relation

$$\Delta x = \sigma c_s \Delta t$$

can be viewed as a CFL condition because $\sigma c_s$ is the largest signal speed in the process.

To write the final scheme in concise form, we first go over from density to pressure by multiplying $\rho$ with $c_s^2$. The values of $p^n$ and $\mu^n = u^n/c_s$ in the nodes $x_i$ of the hexagonal lattice are denoted $\rho_i^n, \mu_i^n$ and the neighboring points of $x_i$ are abbreviated

$$x_{N_{il}} = x_i - \triangle x e_l, \qquad l = 0, \ldots, 6.$$

We end up with the scheme

$$p_i^{n+1} = \sum_{l=0}^{6} f_l^* p_{N_{il}}^n \tilde{\omega}(\mu_{N_{il}}^n; e_l),$$

$$\mu_i^{n+1} = \frac{\sigma}{p_i^{n+1}} \sum_{l=1}^{6} f_l^* p_{N_{il}}^n \tilde{\omega}(\mu_{N_{il}}^n; e_l) e_l.$$

A closer look at the structure of the scheme reveals that it is just a finite difference approximation. Each term in $\tilde{\omega}$ corresponds to a discretized differential operator. For example, the constant 1 in $\tilde{\omega}$ yields an expression in the velocity equation which approximates the pressure gradient

$$-\nabla p(x_i, t_n) \leftrightarrow \sum_{l=1}^{6} f_l^* p_{N_{il}}^n e_l.$$

17

The relation is easily checked by a Taylor expansion around $x_i$. Similarly, one obtains the divergence term in the continuity equation from the linear terms $\sigma \mu \cdot e$ in $\tilde{\omega}$

$$-\operatorname{div}(\rho u)(x_i, t_n) \leftrightarrow \frac{1}{3} \sum_{l=1}^{6} f_l^* p_{N_{il}}^n \mu_{N_{il}}^n \cdot e_l$$

and the quadratic terms in $\tilde{\omega}$ represent discretizations of the nonlinear convective terms. It is interesting to note at this point that the five–velocity distribution (12) with $n = 2$ (velocities in coordinate directions), which has been fallen out of the considerations, would have given rise to standard central differences for gradients and the usual five point stencils for the Laplacian. The additional effort due to the bigger stencils (seven points in the hexagonal case, nine points in case (13)) is not used to increase the accuracy since all approximations are still second order accurate. It might however influence the stability of the scheme which, after all, does not use grid staggering.

To apply the scheme to a given incompressible flow problem the Mach number should be as small as possible, or equivalently, the sound speed $c_s$ should be large. On the other hand, the choice of $c_s$ influences the resolution of the scheme due to the coupling with the time step which is necessary to reproduce the correct kinematic viscosity $\nu$ of the problem. Condition (24) in dimensional quantities with $\lambda = \sigma^2/4$ gives

$$\Delta t = \frac{8\nu}{\sigma^2 c_s^2}. \tag{29}$$

Finally, also the grid length $\triangle x$ is coupled to $c_s$ via the CFL condition

$$\Delta x = \sigma c_s \Delta t = \frac{8\nu}{\sigma c_s}. \tag{30}$$

Altogether, the sound speed can be viewed as a parameter which controls the precision of the scheme. Of course, the numerical cost grows with increasing $c_s$. If we count the time steps necessary to reach a characteristic time $T$ and multiply with the number of grid points in the computational domain of typical length $L$, we can estimate the computing time

$$\text{computing time} \sim \frac{T}{\Delta t} \frac{L^2}{\Delta x^2} \sim \frac{\sigma^4 Re^3}{Ma^4} \tag{31}$$

(we use $Ma = \frac{L}{Tc_s}$ and $Re = \frac{L^2}{T\nu}$). This estimate shows that the schemes are restricted to moderate Reynolds numbers and that the Mach number cannot be chosen too small. Of course, it is tempting to compensate high $Re$ and small $Ma$ numbers with the parameter $\sigma$ to reduce the numerical cost. However, in

18

view of (28), positivity of the distribution function $h$ requires $\sigma^2$ to be larger than $2(Ma^2 + 1)$ which is of order one. Nevertheless, after choosing $c_s$ one would pick $\sigma$ close to its lower bound.

We note that a numerical cost like (31) is typical for explicit finite difference schemes applied to convection diffusion problems. The discretization of the viscous term usually gives rise to a stability bound of the form [23]

$$\frac{\nu \triangle t}{\triangle x^2} = \mathcal{O}(1)$$

and a CFL condition $c_s \triangle t / \triangle x = \mathcal{O}(1)$ is necessary to obtain stability also for convection. Combining the two requirements first yields $\nu / (c_s \triangle x) = \mathcal{O}(1)$ respectively $\triangle x = \mathcal{O}(\nu/c_s)$ which is exactly of the form (30). Inserting the expression for $\triangle x$ in the CFL condition then leads to $\triangle t = \mathcal{O}(\nu/c_s^2)$ which is nothing but (29). Altogether, the numerical cost calculated in (31) is not only found for the Kinetic Scheme but is expected for any finite difference scheme applied to compressible Navier Stokes equations in a low Mach number situation.

In a concrete application, the given divergence free initial velocity field $u^0$ is scaled to obtain $\mu^0 = u^0/c_s$. Then, according to the constant density $\rho$ of the fluid, the average pressure is calculated by multiplying $\rho$ with $c_s^2$. On fixed solid boundaries the no slip condition gives rise to $\mu = 0$. For pressure we use Neumann conditions.

In a first example we consider Hagen Poiseuille flow in two dimensions. Along an infinitely long channel of width $W$ a pressure gradient is applied. It gives rise to a stationary flow with a parabolic velocity profile which is stable for low Reynolds numbers. If the channel stretches in $x_1$ direction and the pressure drop is $\Delta p$ on an $x_1$ interval of length one then the solution has the form

$$u(x) = \begin{pmatrix} u_1(x_2) \\ 0 \end{pmatrix}, \quad u_1(x_2) = \frac{\Delta p}{2\rho\nu}(W - x_2)x_2.$$

where $\rho$ is the density of the fluid and $\nu$ the kinematic viscosity. In our examples we use $W = 1$ and unit density $\rho = 1$. To simulate the infinitely long channel, periodicity for the velocity is assumed at the numerical in and outflow boundaries. The solution is considered stationary if the relative changes in the maximal velocity are less than $10^{-6}$ over a period of 1000 time steps. Choosing a pressure drop $\Delta p = 1$ and $\nu = 0.1$ the theoretical maximal velocity in the channel is

$$u_{\max} = \frac{W^2 \Delta p}{8\rho\nu} = 1.25.$$

19

A calculation with $c_s = 10$ (and hence $Ma \approx u_{\max}/c_s = 0.125$) reproduces the predicted parabolic shape within plotting accuracy (see Figure 3).
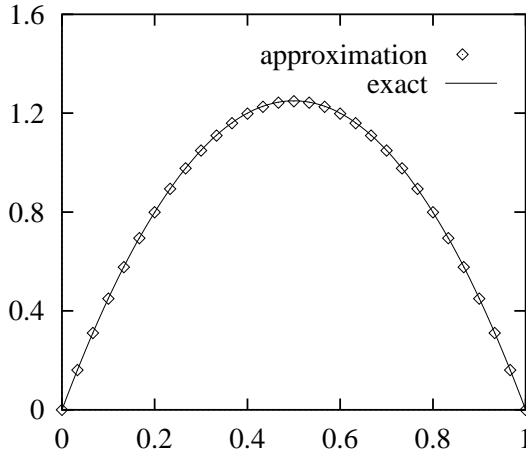


Figure 3: Velocity profile across the channel

For different values of the sound speed $c_s$ the relative error in the maximal velocity is determined. If the Mach number $Ma$ is defined as the quotient between the maximal velocity in the channel and $c_s$ then the error behaves like $\mathcal{O}(Ma^{1.78})$ (taken from the doubly logarithmic plot in Fig. 4).
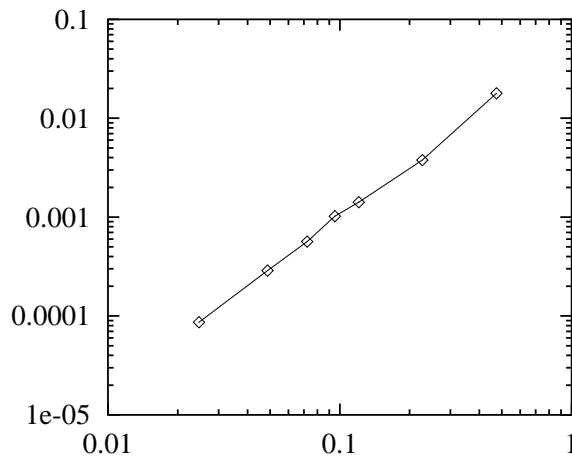


Figure 4: Relative $\mathbb{L}^\infty$ error versus Mach number

Due to the CFL condition, $\Delta x$ is proportional to the Mach number and hence the numerical order of convergence is 1.78 in space. Since $\Delta t$ is proportional to $Ma^2$ the convergence in time is approximately first order, as predicted in Section 4.

In a second test case, we consider driven cavity flow. The incompressible fluid is now bounded by a square enclosure with side length one. A translation

20

of the top with unit velocity generates the fluid motion in the cavity which shows certain vortex phenomena. The reason for choosing this test case is to show that the method also works for more complicated flow simulations (note that the pressure has singularities in the upper corners where the boundary condition for the velocity is discontinuous).

Usually, numerical solutions of cavity flows in two dimensions are based on a vorticity– stream function formulation of the problem. For comparison with results from literature we therefore introduce the stream function $\psi$ which is defined through

$$u = \begin{pmatrix} \frac{\partial \psi}{\partial x_2} \\ -\frac{\partial \psi}{\partial x_1} \end{pmatrix}.$$

Hence, $\psi$ is obtained by integrating $u$ along curves and the value of the integral is independent of the chosen curves only if the integrability condition

$$\operatorname{div} u = \frac{\partial u_1}{\partial x_1} + \frac{\partial u_2}{\partial x_2} = \frac{\partial^2 \psi}{\partial x_1 \partial x_2} - \frac{\partial^2 \psi}{\partial x_2 \partial x_1} = 0$$

is satisfied. Conversely, if $u$ is not divergence free, as in the case of the approximation obtained from the Kinetic Scheme, the stream function is, strictly speaking, not well defined. Practically however, if $\operatorname{div} u$ is very small the dependency on the chosen curves is small. A detailed analysis of this problem is presented in [14] where the cavity flow is calculated with a Lattice Boltzmann method. We will adopt the proposed form

$$\psi(x) = \int_0^1 u_2(x)\, dx_1$$

where the integral from the left to the right edge of the cavity is approximated by a trapezoidal rule based on the given data. We present two results with $Re = 100$ and $Re = 400$. In the first case the Mach number is chosen to be 0.045 and in the second case 0.2. The corresponding number of grids points on the lower edge are 555 respectively 501. The calculations have been performed on an nCUBE 2S with 64 processors. Due to the local structure of the algorithm parallelization is extremely simple. Plots of the stream functions are given in Figure 5 and 6.
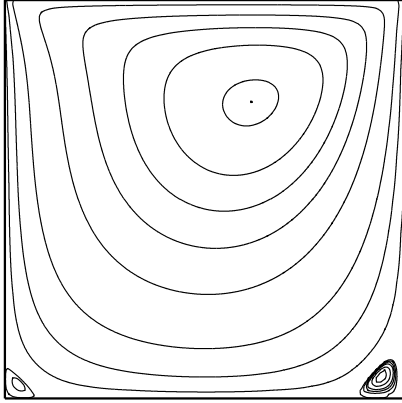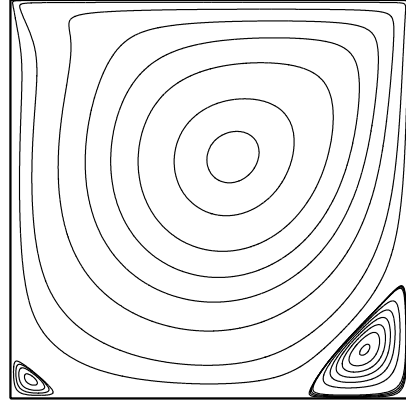
Figure 5: $Re = 100$          Figure 6: $Re = 400$

Strengths and positions of the primary as well as the secondary vortices co-
incide well with results obtained with other methods (taken from the list in
[14]). For comparison, we list the data in table i, ii, and iii. The last row in
each $Re$–block correspond to the results obtained with the Kinetic Scheme.

| $Re$ | article | $\psi_{\max}$ | $x_1$ | $x_2$ | $Re$ | article | $\psi_{\min}$ | $x_1$ | $x_2$ |
|------|---------|---------------|-------|-------|------|---------|---------------|-------|-------|
| 100  | [31]    | 0.1034        | 0.619 | 0.738 | 100  | [31]    | -1.94e-6      | 0.038 | 0.031 |
|      | [10]    | 0.1034        | 0.617 | 0.734 |      | [10]    | -1.75e-6      | 0.031 | 0.039 |
|      | [30]    | 0.1033        | 0.617 | 0.741 |      | [30]    | -2.05e-6      | 0.033 | 0.025 |
|      | [14]    | 0.1030        | 0.620 | 0.737 |      | [14]    | -1.72e-6      | 0.039 | 0.035 |
|      |         | 0.1030        | 0.616 | 0.737 |      |         | -1.66e-6      | 0.030 | 0.040 |
| 400  | [31]    | 0.1136        | 0.556 | 0.600 | 400  | [31]    | -1.46e-5      | 0.050 | 0.050 |
|      | [10]    | 0.1139        | 0.554 | 0.606 |      | [10]    | -1.42e-5      | 0.051 | 0.047 |
|      | [30]    | 0.1130        | 0.557 | 0.607 |      | [30]    | -1.45e-5      | 0.050 | 0.043 |
|      | [14]    | 0.1121        | 0.560 | 0.608 |      | [14]    | -1.30e-5      | 0.055 | 0.051 |
|      |         | 0.1123        | 0.555 | 0.605 |      |         | -1.33e-5      | 0.050 | 0.047 |

Table i: Primary vortex          Table ii: Lower left vortex

| $Re$ | article | $\psi_{\min}$ | $x_1$ | $x_2$ |
|------|---------|---------------|-------|-------|
| 100  | [31]    | -1.14e-5      | 0.938 | 0.056 |
|      | [10]    | -1.25e-5      | 0.945 | 0.063 |
|      | [30]    | -1.32e-5      | 0.942 | 0.050 |
|      | [14]    | -1.22e-5      | 0.945 | 0.063 |
|      |         | -8.30e-6      | 0.939 | 0.051 |
| 400  | [31]    | -6.45e-4      | 0.888 | 0.119 |
|      | [10]    | -6.42e-4      | 0.891 | 0.125 |
|      | [30]    | -6.44e-4      | 0.886 | 0.114 |
|      | [14]    | -6.19e-4      | 0.890 | 0.126 |
|      |         | -6.11e-4      | 0.885 | 0.121 |

Table iii: Lower right vortex

Finally, we want to give a few remarks concerning the computational effort. Since the restrictions on the time step are similar to those known for explicit finite difference schemes, the Kinetic Scheme in its present form can certainly not compete with implicit methods. Also, the kinematic viscosity restricts the grid size in a way which is not acceptable in practice. By adding viscous terms to the distribution function $h$, the latter problem can be removed. Also, the critical pressure terms in the scheme can treated implicitly, giving rise to a pressure correction method. While these modifications are presently studied, the main idea of the considerations here is to analyze the behavior of Kinetic Schemes in low Mach number situations. Moreover, as we will show in the next section, the Kinetic Scheme in the present form gives some insight into the Lattice Boltzmann method which has not been mentioned before.

# 6 Connection to LB methods

The Lattice Boltzmann (LB) approach is a relatively new method to study transport phenomena like fluid motion governed by Navier–Stokes equations. It relies on the observation that a simulation of a strongly simplified, microscopic gas model can nevertheless reproduce a meaningful, macroscopic behavior. Similar to classical discrete ordinate methods for the Boltzmann equation [16], the microscopic velocities are restricted to a finite set. By discretizing time and space compatibly to these velocities a simple, discrete dynamical system is obtained. In a first approach, the Liouville equation for the discrete gas has been solved directly, giving rise to so called lattice gas automata (LGA) [8, 9]. An advantage of these methods is the possibility of a very effective implementation on parallel computers. However, there are some inherent problems with LGA which can be avoided by considering the Boltzmann equation for the

23

model gas instead of the Liouville equation [20]. In particular, if the Boltzmann collision operator is replaced by a single relaxation time approximation (BGK) the resulting method becomes very flexible [5, 25]. In the following, we will show that these so called Lattice Boltzmann BGK models are closely related to the Kinetic Scheme presented in Section 5.

To fix notation, let $c_i$ denote the discrete velocities in the model and $f_i(x, t)$ the single–particle distribution function for the velocity $c_i$ at lattice node $x$ and time $t$. The Lattice Boltzmann BGK equation then has the form

$$\frac{1}{\Delta t} \left( f_i(x + c_i \Delta t, t + \Delta t) - f_i(x, t) \right) = -\frac{1}{\tau} \left( f_i(x, t) - f_i^{eq}(x, t) \right). \qquad (32)$$

A fundamental restriction on the velocities $c_i$ is their compatibility with a regular space lattice in the sense that the lattice must be invariant under $\Delta t c_i$–translations. The relaxation term on the right hand side is called BGK collision operator. The time scale on which the collision term relaxes the distribution function $f_i$ towards $f_i^{eq}$ (the equilibrium distribution) is controlled by the parameter $\tau > 0$. Moreover, the conservation property

$$\sum_i \begin{pmatrix} 1 \\ c_i \end{pmatrix} (f_i - f_i^{eq}) = 0 \qquad (33)$$

is assumed, which implies that density $\rho$ and momentum $\rho u$ corresponding to $f_i$ and $f_i^{eq}$ coincide. It is therefore natural to assume that the $(x, t)$–dependence of $f_i^{eq}$ enters implicitly through the parameters

$$\begin{pmatrix} \rho \\ \rho u \end{pmatrix} = \sum_i \begin{pmatrix} 1 \\ c_i \end{pmatrix} f_i. \qquad (34)$$

Under certain assumptions on $f_i^{eq}$ a Chapman Enskog expansion of (32) together with a low Mach number assumption shows that the average velocity $u$ defined in (34) is an asymptotic solution of the incompressible Navier Stokes equation [14]. The viscosity turns out to be directly connected to the relaxation parameter $\tau$.

In order to relate the Lattice Boltzmann approach to Kinetic Schemes, we recall that a Kinetic Schemes can be viewed as a sequence of free flow steps where, at the beginning of each step, the constraint $f(x, v, t) = h(\rho(x, t), u(x, t); v)$ is enforced. Thus at time $t + \triangle t$, we have

$$f(x, v, t + \triangle t) = h(\rho(x - v \triangle t, t), u(x - v \triangle t, t); v).$$

24

If $h$ is a discrete velocity distribution (like (27)), we find that also $f$ is discrete

$$h(\rho(x - v\triangle t, t), u(x - v\triangle t, t); v)$$

$$= \sum_{i=0}^{6} h_i(\rho(x - c_i\triangle t, t), u(x - c_i\triangle t, t))\delta(v - c_i)$$

$$= \sum_{i=0}^{6} f_i(x, t + \triangle t)\delta(v - c_i).$$

and we can remove the fixed $\delta$-measures in the description of the evolution

$$f_i(x, t + \triangle t) = h_i(\rho(x - c_i\triangle t, t), u(x - c_i\triangle t, t)).$$

A change of variables $x - c_i\triangle t \mapsto x$ finally yields

$$f_i(x + c_i\triangle t, t + \triangle t) = h_i(\rho(x, t), u(x, t)).$$

Identifying $f_i^{eq}$ with the equilibrium distribution $h_i(\rho, u)$ we see that the Kinetic Scheme can be regarded as LB method (32) with $\tau = \triangle t$. (We remark that the equilibrium distribution based on $h_i(\rho, u)$ from Section 5 has the same form as the one described in [5] and that the approach in Section 3 based on the nine velocity distribution (13) leads to the known square lattice method [1, 14].) Conversely, the LB method can be considered as a linear combination of a Kinetic Scheme and a free flow solver. Indeed, using the splitting

$$f_i(x + c_i\Delta t, t + \Delta t) = \left(\frac{\triangle t}{\tau} + \left[1 - \frac{\triangle t}{\tau}\right]\right) f_i(x + c_i\Delta t, t + \Delta t)$$

in the LB evolution (32) we find the equivalent formulation

$$\left(1 - \frac{\triangle t}{\tau}\right)(f_i(x + c_i\Delta t, t + \Delta t) - f_i(x, t))$$

$$+ \frac{\triangle t}{\tau}(f_i(x + c_i\Delta t, t + \Delta t) - f_i^{eq}(x, t)) = 0. \quad (35)$$

Only in the case $\tau = \triangle t$, the evolution is exactly equal to the one of the Kinetic Scheme. Since

$$f_i(x + c_i\Delta t, t + \Delta t) - f_i(x, t) = 0$$

yields the exact solution to the free flow problem $\partial_t f_i + c_i \cdot \nabla f_i = 0$, the other contribution to (35) can be interpreted as a free flow solver. In any case, the Kinetic Scheme is an important building block of the Lattice Boltzmann

25

method. Since it works directly on the variables $(\rho, u)$ of the problem (and is actually a finite difference scheme for $(\rho, u)$ as described in Section 4), this part of (35) is well understood. The free flow part, however, introduces variables which do not have a direct counterpart in the actual Navier Stokes problem (there are, for example, seven occupation numbers $f_i$ in the hexagonal case versus three variables $\rho, u_1, u_2$ in the equations).

# 7  Conclusion

We have investigated how Kinetic Schemes for the isentropic Euler system behave in the case of low Mach numbers. It turns out that they approximate solutions of the incompressible Navier–Stokes equation where the Reynolds number is controlled by the limit of the ratio $\triangle t / Ma^2$. To enhance the performance of the scheme the freedom in the choice of the microscopic velocity distribution is used. In particular, discrete distribution functions which are expanded at low Mach numbers lead to simple schemes which can be regarded as explicit finite difference discretizations. Since the Lattice Boltzmann method can be written as a linear combination of a Kinetic Scheme and a free flow solver, the investigations also give a new perspective on LBM.

In the present form, the numerical cost of the Kinetic scheme in 2D grows with $Re^3$ so that applications are practically restricted to moderate Reynolds numbers. Also, compressibility effects cannot be arbitrarily reduced because the Mach number, which should be as small as possible, enters like $Ma^{-4}$ in the numerical cost. These restrictions, however, are to be expected for any explicit finite difference scheme applied to compressible Navier–Stokes equations in a low Mach number case (and also for LBM due to its closeness to Kinetic Schemes). Modifications of the presented scheme to remove the restrictions coming from the purely explicit treatment as well as the correlation between grid size and Reynolds number are possible and will be considered in future work. The often quoted advantage of LBM to be easily parallelizable also applies to the Kinetic scheme in the present form. In fact, it holds for any explicit finite difference scheme.

# 8  Acknowledgements

26

# References

[1] T. ABE, *Derivation of the Lattice Boltzmann Method by Means of the Discrete Ordinate Method for the Boltzmann Equation*, J. Comput. Phys. 131, 241-246, 1997

[2] M. BÄCKER, K. DRESSLER, *A kinetic method for strictly nonlinear scalar conservation laws*, ZAMP, Vol.42, 1991

[3] A. J. CHORIN, J. E. MARSDEN, *A Mathematical Introduction to Fluid Dynamics*, Springer, 1979

[4] C. CERCIGNANI, *The Boltzmann Equation And Its Applications*, Springer, 1988

[5] H. CHEN, S. CHEN, W. MATTHAEUS, *Recovery of the Navier-Stokes equations using a lattice-gas Boltzmann method*, Phys. Rev. A 45, R5339, 1992

[6] F. CORON, B. PERTHAME, *Numerical passage from kinetic to fluid equations*, SIAM J. Numer. Anal., 28, 26–42, 1991

[7] S. M. DESHPANDE, *Kinetic theory based new upwind methods for inviscid compressible flows*, AIAA paper 86–0275, American Institute of Aeronautics and Astronautics, New York, 1986

[8] G. DOOLEN ED., *Lattice Gas Methods for Partial Differential Equations*, Addison Wesley, 1990

[9] U. FRISCH, B. HASSLACHER, Y. POMEAU, *Lattice–Gas Automata for the Navier–Stokes Equation*, Phys. Rev. Lett. 56, 1505, 1986

[10] U. GHIA, K. N. GHIA, C. Y. SHIN, *High-Re solutions for incompressible flow using the Navier-Stokes equations and a multigrid method*, J. Comput. Phys. 48, 387-411, 1982

[11] Y. GIGA, T. MIYAKAWA, *A kinetic construction of global solutions of first order quasilinear equations*, Duke Math. J., 50, 505–515, 1983

[12] A. HARTEN, P. D. LAX, B. VAN LEER, *On upstream differencing and Godunov–type schemes for hyperbolic conservation laws*, SIAM Rev., 25,35–61, 1983

[13] C. HIRSCH, *Numerical computation of internal and external flows*, Vol. 1, Wiley, 1998

[14] S. Hou, Q. Zou, S. Chen, G. Doolen, A. C. Cogley, *Simulation of Cavity Flow by the Lattice Boltzmann Method*, J. Comput. Phys. 118, 329, 1995

[15] S. Kaniel, *Approximation of the hydrodynamic equations by a transport process*, in Proceedings of IUTAM Symposium on Approximation Methods for Navier–Stokes Problems, Lecture Notes in Math. 771, R. Rautmann, ed., Springer–Verlag, Berlin, New York, 1980

[16] R. Illner, T. Platkowski, *Discrete velocity models of the Boltzmann equation: A survey on the mathematical aspects of the theory*, SIAM Rev. 30, 213-255, 1988

[17] M. Junk, *Kinetic Schemes: A new Approach and Applications*, Ph.D. thesis, Universität Kaiserslautern, Shaker Verlag, 1997

[18] S. Kaniel, *A Kinetic Model for the Compressible Flow Equation*, Indiana Univ. Math. J., Vol.37, No.3, 1988

[19] P. L. Lions, B. Perthame, E. Tadmor, *A kinetic formulation of multidimensional scalar conservation laws and related equations*, J. Amer. Math. Soc., 7, 169–191, 1994

[20] G. R. McNamara, G. Zanetti, *Use of the Boltzmann Equation to Simulate Lattice–Gas Automata*, Phys. Rev. Lett. 61, 2332, 1988

[21] B. Perthame, *Boltzmann type schemes for gas dynamics and the entropy property*, SIAM J. Numer. Anal. 27, No.6, 1405-1421, 1990

[22] B. Perthame, E. Tadmor, *A kinetic equation with kinetic entropy functions for scalar conservation laws*, Comm. Math. Phys., 136, 501–517, 1991

[23] R. Peyret, T. D. Taylor, *Computational Methods for Fluid Flows*, Springer, 1983

[24] D. I. Pullin, *Direct simulation methods for compressible inviscid ideal–gas flow*, J. Comput. Phys., 34, 231–244, 1980

[25] Y.H. Qian, D, d'Humieres, P. Lallemand, *Lattice BGK-Modell for Navier-Stokes Equation*, Europhys. Lett. 17, 479, 1992

[26] M. B. Reider, J. D. Sterling, *Accuracy of Discrete–Velocity BGK Models for the Simulation of the Incompressible Navier–Stokes Equations*, Computers & Fluids 24, 459, 1995

[27] J. RIVLIN, S. KANIEL, *Numerical solution of the equation of compressible flow by a transport method*, Numerical Methods for Partial Differential Equations, 6, 245–261, 1990

[28] R. D. REITZ, *One–dimensional compressible gas dynamic calculations using the Boltzmann equation*, J. Comput. Phys., 42, 108–123, 1981

[29] R. H. SANDERS, K. H. PRENDERGAST, *On the origin of the 3 kiloparsec arm*, Astrophys. J., 188, 489-500, 1974

[30] R. SCHREIBER, H. B. KELLER, *Driven cavity flows by efficient numerical techniques*, J. Comput. Phys. 49, 310-333, 1983

[31] S. P. VANKA, *Block-implicit multigrid solution of Navier-Stokes equations in primitive variables*, J. Comput. Phys. 65, 138-158, 1986